Journal of Advances and Scholarly Researches in Allied Education
Vol. 20, Issue No. 2, April-2023, ISSN 2230-7540

Structural Characterization of Metal free Organic Dyes Sensitized Solar Cell(Dssc)theory for Harvesting System

Meghmala Vaijanath Ingole[1]* Dr. Sumit Kumar Gupta[2]

[1] Research Scholar, University Of Technology, Jaipur, Rajasthan.

[2] Professor, Dept. of Physics. University Of Technology, Jaipur, Rajasthan

Abstract - Density functional theory (DFT) and time-dependent density functional theory (TD-DFT) calculations were carried out to ascertain whether or not certain new metal-free 1,3,4-oxadiazole compounds O1-O7 may serve as metal-free organic dyes in the application of dye-sensitized solar cells (DSSCs). The relative efficiency of the compounds as dyes in DSSCs were determined by analyzing their electron contributions, hole contributions, and electron-hole overlaps, with an emphasis on the electron densities on the anchoring segments. The charge separation distance (r) and the electron-hole overlap () were studied because excitations cause charge transfer (CT), and because transition density matrices (TDM) describe the separation of each electron from its corresponding hole. Electron excitation processes may be described by a number of parameters such as the diffusion constant (D) and the electron lifetime (t). Since O3 had the highest IPCE value, it was deemed to be the most efficient dye.

Keywords - DFT; TD-DFT; DSSCs; donor; π-spacer; acceptor

----------X----------

INTRODUCTION

The ever-increasing requirement for energy to sustain human life has always been a driving force behind technological development. To yet, most energy products have relied on fossil fuels like petroleum, natural gas, and coal as their primary source of energy. Petroleum is employed in a wide variety of applications. Climate change and global warming are exacerbated by the emissions of greenhouse gases from fossil fuels. As a result, there is a growing need for alternative energy sources, such as solar and wind power, that don't harm the environment as much as fossil fuels do.

Both global population and energy consumption have been on the rise. Because of this, increased power demand calls for more eco-friendly renewable energy sources. Renewable energy is safe for the planet. Wind, solar, hydropower, geothermal, and biomass, which are the most prevalent renewable energy sources, are nonpolluting and have an infinite supply of potential to generate electricity. The sun is the source of all renewable energy. Many scientists throughout the globe have recently been interested in alternative energy sources.

Depending on its design, wind turbines may generate anywhere from 600 kilowatts (kW) to 9 megawatts (MW) of rated electricity Wind turbines can harness this air movement to create energy. When compared to other forms of energy production, wind power's low cost really stands out. Wind farms have a set price, but may be used for over 20 years with no further costs for energy. Farmers and ranchers in the countryside have access to a steady economy that supports their work around the clock. Most wind power is produced in rural areas not in urban centers where it would cause noise and visual pollution and, in rare cases, harm local wildlife.

The photovoltaic effect is what gives solar cells their ability to generate electricity. The great efficiency of these solar cells has made them widely accessible. Thin-film solar cells (TFSCs) and thin-film photovoltaic cells (TFPVs) are the next generation of solar panels. Materials like Copper Indium Gallium Selenide (CIGS), Cadmium Telluride (CdTe), micro amorphous silicon, and amorphous silicon have shown to be the most effective for use in thin film solar cells. The cheap price and adaptability of these cells over those of earlier generations are huge advantages. Third-generation technology includes Dye-Sensitized Solar Cells O'Regan & developed the DSSC. Dye-sensitized solar cells, quantum-dot solar cells, organic solar cells, multi-junction solar cells, nanocrystalline nanowire cells, and polymer solar cells are all examples of the latest generation of solar cells. The third-generation solar cell with the most advanced technology is the dye-sensitized cell. DSSCs are inexpensive solar cells that are both

environmentally benign and very adaptable throughout the production process.

A kind of thin film solar cell known as a dye-sensitized solar cell. A semiconductor substrate forms the backbone of the DSSC. The photo-sensitized anode, metal oxide semiconductor, electrolyte, counter electrode material, and transparent conducting substrate are the DSSC's five main components. There are two types of dye-sensitized solar cells: those that use metal and those that don't. They are efficient in converting electricity.

LITERATURE REVIEW

Tao Hua et al. (2019) created two new organic colors based on phenothiazine that don't need any metals. The molecular structures of PH2 and PH3 dyes are D-D--A; these dyes include two donor groups, an acceptor group formed from cyanoacedic acid, and a bridge conjugation group formed from thiophene. Enclosed insulated molecular wire (EIMW) molecules are what PH2 and PH3 dyes are. When compared to PH1 dye, both of these dyes do a better job of preventing dye clumping. The PH2, PH3, and PH1 dye encased insulated molecular wire (EIMW) forms a stiff circular chain. Compared to PH1 (5.64%) and PH3 (6.51%), the power conversion efficiency of PH2 dye (7.08) was much higher. Chenodeoxycholic acid (CDCA), a co-adsorbent, was included into the dyes (PH1, PH2, and PH3). The power conversion efficiencies (PH1 - 7.91 %, PH2 - 7.8 %, and PH3 - 7.5 %) were improved when the dyes were added (dye + CDCA). According to the findings, DSSCs with EIMW incorporated into organic dyes had higher PCE.

Ahmad Irfan et al. (2019) constructed and reconstructed The optical, electrochemical, and DSSCs applications of four distinct triphenylamine and carbazole based metal free organic dyes were studied. In each of the four dyes (Dye 1, Dye 2, Dye 3, and Dye 4), the donor unit is either triphenylamine or carbazole, the bridge unit is pyridine, and the acceptor unit is cyanoacetic acid. Higher red shifted, absorption bands, and short-circuit photocurrent density (JSC) are characteristics shared by the di-substituted donor moieties of Dye 2 (triphenylamine) and Dye 4 (carbazole) dye sensitizers.

Hyeonjun Jeong et al. (2018) looked at two novel metal-free organic dyes based on phenothiazine. Carboxylic acid (MPhe-ind) and cyanoacetic acid (BPhe-ind) are two examples of differan acceptors. Conjugation through -bridge of a carboxylated 1,3-indanedione unit. Absorption occurs between 2.10 and 2.67 microns (MPhe-ind and BPhe-ind, respectively). Gaussian 09, a quantum chemistry software, was used to evaluate computational investigations of MPhe-ind and BPhe-ind. Power conversion efficiency is poor for both the MPhe-ind (1.88%) and BPhe-ind (2.49%) dyes. Dye removal efficiency (PCE) was increased to 1.95% and BPhe-ind removal efficiency (PCE) was increased to 2.58% when the co-adsorbent chenodeoxycholic acid (CDCA) was also added. Both the MPhe-ind PCE (2.10%, Jsc 6.12 mA cm-2) and BPhe-ind PCE (2.67%, Jsc 7.61 mA cm-2) were unaffected by the addition of co-adsorbent palmitic acids (PA) to the dyes.

Muhammed Yoosuf et al. (2019) Both TPAA6 and TPAA7, which are based on anthracene, are metal-free organic sensitizers. Triphenylamine serves as the donor in both TPAA6 and TPAA7, while cyanoacidic acid is the acceptor and benzene and anthracene serve as the -bridge units. Both of these dyes have a D-A-based structure and a triple bond rigidified anthracene-triphenylamine connection. Light up to 600 nm may be harvested using the TPAA6 and TPAA7 sensitizers. Power conversion efficiency for the dye-sensitized solar cell was 3.56 percent for TPAA6 and 4.38 percent for TPAA7. In order to aggregate on the TiO2 surface, the sensitizers TPAA6 (Jsc of 9.35 mA cm2, Voc of 593 mV, FF of 0.64%) and TPAA7 (Jsc of 10.93 mA cm2, Voc of 629 mV, FF of 0.63%) both have a propeller-shaped structure. Two anthracene units include the TPAA7 sensitizers, allowing for more efficient power conversion.

Zhi-Sheng Wu et al. (2019) Both dyes were developed and manufactured specifically for use in DSSC. The triphenylamine sensitizers (D8 and D9) rely on the alkylphenyl/alkyloxy phenyl-containing bithiophene. This cyclic thiourea-functionalized triphenylamine donor unit includes 2-cyanoacrylic acid as the acceptor unit. The D7 dye (4,4′-dihexyl-2,2′- bithiophene spacer) is made and compared to another dye and another dye. The conjugated system (aromatic alkylphenyl/alkyloxy phenyl) led to an increase in absorption bands (440nm, 463nm, and 482nm) and a red shift in comparison to the aforementioned three dyes (D7, D8, and D9). The D8 dye has a higher efficiency in converting electricity (7.88%) than the D7 and D9 alternatives (7.41% and 7.72%).

RESEARCH METHODOLOGY

Computational Details

Gaussian 09 version E01 [38] was used for all computations. For both the DFT and TD-DFT simulations, the molecular geometries were optimized in the gas phase. The M06-2X/6-31G(d,p) theory level was used for optimization of all structures. In the past, researchers have shown that the M06-2X functional produced almost spot-on electronic excitation energies for main-group thermochemistry Frequency calculations were performed alongside the optimization process to ensure that the structures' energy requirements were minimized. To study the ICT at the same level of theory, we used the optimized structures of the organic dyes labeled O1-O7 to perform TD-DFT calculations in the gas phase and then analyzed their frontier molecular orbital natures (FMO) with multi wfn software. Single point calculations using conceptual density functional theory (CDFT) and molecular electrostatic potentials (MEPs) were also

performed to determine molecular orbital structures and HOMO and LUMO energies, in addition to the optimized structures.

DATA ANALYSIS

OPTIMIZED GEOMETRY

A molecule's projected behavior is very sensitive to how well its optimal structure is determined. Each structure has to go through a series of optimization stages to get to its least energy configuration, also known as the optimized structure. Frequency calculations confirmed that the optimized structures were true minima or transition states. Higher-order saddle points are ascribed to structures with two or more imaginary frequencies, whereas transition states are used to describe structures with a single imaginary frequency as a result, it is widely agreed that an optimally optimized structure has no negative frequency and has attained its lowest energy. Negative vibrational frequencies in the range of 10–100 cm1 may often be disregarded, however extremely big, flabby molecules are an exception to this rule.

COULOMB ATTRACTIVE ENERGY AND ELECTRON EXCITATION ANALYSES

The electro-optical characteristics and electron-hole pair dissociation potential of the metal-free organic dye determine the DSSC's efficiency. Binding (Coulomb attractive) energy keeps the electron in its hole due to the existence of Coulombic interactions between electron-hole pairs. Organic molecules have a high binding energy because the Coulombic force between the electron-hole pair is strong due to the low dielectric constant of organic molecules. The second scenario results in the electron leaving its hole. The relationship among binding energy, band gap energy, and single point excitation energy is given by Equation.

$$E_b = E_{(LUMO\text{-}HOMO)} - E_{(S1\text{-}S0)}$$

where E(LUMO-HOMO) is the band gap energy, E(S1-S0) is the single point excitation energy between the ground and the excited state, and Eb is the binding energy, which may alternatively be thought of as an approximation of the dissociation energy of excitation. An electron needs a positive single point energy to be effectively stimulated to the LUMO level. This also helps to disentangle it from its crater. Foretelling the electron-hole transport barrier is the ionization potential (IP) and electron affinity (EA). The latter may be determined with the help of Equation:

$$IP = -E_{(N-1)} - E_N$$

The equation allows for the determination of the latter:

$$EA = -E_N - E_{(N+1)}$$

where N is the state of an electron. The E(LUMO)-(HOMO) energy gap was previously thought to be a good proxy for IP [44]. However, a recent investigation by Bulat et al. demonstrated the crucial roles played by electron energies in certain atomic or molecular orbitals during excitation events. No matter which molecular orbitals an electron occupies, it always has a fixed location inside the molecule's volume. The overall electronic density is denoted by, whereas the average orbital energy is denoted by, if each orbital i has a density of electrons equal to i (r) and an energy of i.

$$\bar{\varepsilon}(r) = \frac{\sum \rho_i(r)\varepsilon_i}{\rho(r)}$$

When Equation is multiplied by each occupied orbital, the result is:

$$\overline{I(r)} = \frac{\sum \rho_i(r)|\varepsilon_i|}{\rho(r)}$$

where I(r) is the mean ionization energy in the immediate region at a distance r. I(r) is the typical energy needed to eject an electron from a molecule or atom at location r. The lowest I(r) values correlate to the most energetic, loosely bound electrons inside an atom or molecule. According to Fukui's logic, these are the most probable locations for protonation, free radical assault, and electrophilic substitution. Important molecular features such kinetic energy density, local temperature, local polarizability/hardness, electronegativity, atomic shell structure, and electrostatic potential were demonstrated to be connected to I(r). When Bulat et al. [45] the I(r) of 12 different compounds, they found that only 5 of them had electrons in the HOMO state. Increased polarity in the excited state results from the non-symmetrical distribution of electrons that occurs during excitation. The dipole moment provides a quantitative measure of the degree to which the polarity of a molecule affects its geometry. Therefore, the dipole moment is directly proportional to the opposite sign of the molecule's symmetry. To get excited, an electron must first absorb a photon. Absorption probabilities for photons increase as their oscillator strengths (f) increase. Electrons will eventually settle back to the ground state from the excited one since the former is less stable. Single point excitation energies are positive for all chemicals in Table 1 except for O7. Therefore, electrons will get excited in the vast majority of compounds. O5 has the greatest single point energy, suggesting that one electron in this molecule may be stimulated more readily than in the others. The problem is that its f is lower than O2's. O4 is extremely symmetric due to its low dipole moment, and its electron can more quickly return to its ground state after being excited than in the other compounds.

Table 1. Electron excitation parameters of each molecule

Compound	HOMO (eV)	LUMO (eV)	$E_{(LUMO-HOMO)}$ (eV)	E_b (eV)	$E_{(S1-S0)}$ (eV)	μ (Debye)	f	ε_{abs} ($L \cdot mol^{-1} \cdot cm^{-1}$)	λ_{max} (nm)	IP (eV)	EA (eV)
O1	−6.95	−2.59	4.36	3.72	0.64	7.48	0.545	27,692	337	6.69	2.00
O2	−7.37	−2.15	5.22	4.50	0.72	2.81	1.030	41,649	356	7.45	1.49
O3	−7.23	−2.17	5.06	4.17	0.89	5.73	0.853	34,505	360	7.75	0.48
O4	−7.59	−2.12	5.47	4.23	1.23	0.91	0.675	28,404	325	7.63	1.44
O5	−7.39	−2.45	4.94	3.37	1.57	6.66	0.782	37,278	325	5.52	4.17
O6	−6.69	−2.95	3.74	3.43	0.31	3.18	0.042	3522	429	5.28	4.26
O7	−7.06	−2.58	4.48	4.65	−0.17	5.12	0.380	15,470	496	4.65	5.00

According to the dipole moment, O4 should be the least soluble and O1 should be the most soluble in polar liquid. These compounds are predicted to exhibit an increase in wavelengths upon dissolution as a result of their interaction with molecules of the solvent. IP and EA are shown to be correlated as IP rises, EA falls. This makes sense given that removing an electron from an atom's energy state through IP uses energy, while gaining an electron via EA releases energy. Table 1 shows the EA rankings, which go as follows: O7 > O6 > O5 > O1 > O2 > O3 > O4. All of the compounds have the ability to effectively transfer electrons into the conduction band edge once activated since their LUMO energies are higher than the published value of the conduction band edge of TiO2 (4.21 eV). Their electrons are also able to be effectively regenerated into the dye because their HOMO energies are lower than the published value of the HOMO energy (4.6 eV) of I /I 3 None of the chemicals, save O6 and O7, absorb light in the visible or NIR spectrum.

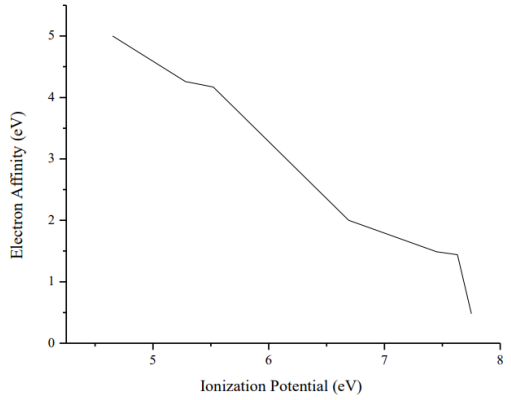

Figure 1. Relationship between ionization potential and electron affinity for the 1,3,4-oxadiazole compounds

Molecular Electrostatic Potential (MEP)

In order to obtain the electronegativities of selected atoms (Table 2), molecular electrostatic potential (MEP) calculations were performed because they have been shown to be a reliable chemical descriptor for measuring electronegativities of atoms in a molecule that are comparable to experimental observations [46]. Electronegativities measured by MEP point to either nucleophilic or electrophilic assaults, with positive values indicating the former and negative ones the latter. Since CN and COOH anchoring segments play such a crucial role in electron injections into the semiconductor's conduction band edge, we shall focus only on their electronegativities. According to Table 2, the highest concentration of electrons is found in the combination of the nitrogen atom (N15) of the cyano anchoring segment with the oxygen atoms (O17 and O18) of the carboxylic acid anchoring segment in O1, while the lowest concentration of electrons is found in the nitrogen atom (N53) of the cyano anchoring segment in O7. O1 > O5 > O2 > O3 > O4 > O6 > O7 describes a pattern of MEP values. Due to its very low EA value, O7 was predicted to have the lowest electronegativity value.

Table 2. Electronegativities on the anchoring segments obtained through molecular electrostatic potentials (−1 × 103).

Compound	Atoms N15	O17	O18	N25	N27	N28	O27	O28	O29	O30	O31	N53	N182	O184	O185
O1	235	349	414												
O2					246				364	362					
O3						251				308	411				
O4				229			327	400							
O5	233	341	402												
O6													206	288	412
O7												86.6			

3.3. Photovoltaic Parameters

In order to discriminate between donor, -spacer, and acceptor fragments, MEP examines the electron densities of atoms inside the molecule; the acceptor fragment has the largest concentration of electrons. (See ESI for a more in-depth explanation of the atomic-level electron-hole analysis). Stoke's Equation may be used to determine the diffusion constant D by which electrons move from the acceptor fragment's anchoring groups into TiO2's conduction band.'

$$D_\pi = \frac{K_B T}{6\pi\eta r_{dye}}$$

where KB is Boltzman's constant; = the medium's viscosity, which may be assumed to be He at 300 K (20.0 106 Pas) here as the studies were conducted in the gas phase; Dye molecular radii are denoted by rdye, where NA is Avogadro's number. The latter is derived using Equation.

$$r_{dye} = a = \sqrt[3]{\frac{3M}{4\pi\rho NA}}$$

NA = Avogadro's number, M = dye molecular weight, = He gas density (9.00 102 kgm3) at STP, and a = Onsager cavity radii. As was previously mentioned, the diffusion constant is crucial in reducing the likelihood of charge recombination during excitations (faster diffusing electrons have a less chance of recombining). O2 and O4 have the largest D (Table 3) due to their low molecular weights. Therefore, their photoelectrons will diffuse more quickly into TiO2's conduction band because of their tiny sizes compared to those of the other compounds. Charge is accumulated as electrons diffuse towards TiO2's conduction band. The charge collection efficiency (ncollect) is calculated using Eq. and measures how well charges are collected.

$$n_{collect} = \frac{D_\pi}{(\delta_p)^2}$$

where δp represents the dye's LUMO potential minus the TiO2 conduction band. ncollect is a pre-injection electron availability measurement tool. In comparison to the other chemicals, O3 has the highest charge accumulation over its ncollect value because of its high LUMO excited-state energy. In O6, charge does not accumulate because the potential difference between the LUMO excited state energy and the conduction band of TiO2 is small.

Table 3. Photovoltaic parameters of compounds that were tested as organic dyes

Compound	τ_{dye} (m) (1×10^{-7})	D_π (1×10^{-11})	δ_p	$n_{collect}$ (1×10^{-12})	LHE	t (s) (1×10^{-38})	Φ_{inj}	IPCE (1×10^{-12})	ΔG^{regen}_{dye} (eV)
O1	1.62	6.73	−6.08	1.68	0.715	0.212	0.795	1.21	2.35
O2	1.15	9.51	−5.64	2.99	0.907	0.120	1.00	2.33	2.77
O3	1.16	9.47	−5.66	2.96	0.860	0.148	1.00	2.55	2.63
O4	1.15	9.51	−5.61	3.02	0.789	0.154	0.961	2.29	2.99
O5	1.41	7.73	−5.94	1.51	0.835	0.136	0.849	1.55	2.79
O6	1.89	5.76	−6.44	1.39	0.0922	4.56	0.480	0.0615	2.09
O7	1.54	7.07	−6.07	1.92	0.583	0.633	0.996	1.11	2.46

The spectral distribution of the sunlight received by the molecule is quantified by the light harvesting efficiency (LHE), which may be written as:

$$LHE = 1 - 10^{-f}$$

where f is the strength of the oscillator in the dye molecules. Equation shows that when the oscillator strength is high, the LHE will also be strong. O2 has a significant LHE because its f value is so high. If the efficiency with which stimulated electrons are injected (Φinj) assumes that the fluorescence emission factor of the dye is equal to one. (Φf), So, we may use Equation to define the latter:

$$\Phi_f = \frac{I\varepsilon_{em}}{I\varepsilon_{abs}}$$

where the regions beneath the emission and absorption spectra are represented by the integrated emission and absorption coefficients, Iem and Iabs. Extrapolation of absorption spectra yields the former The huge discrepancy between the O3 absorption spectrum and emission spectrum Φinj exhibits in this building. This means that more photoelectrons can be moved from the LUMO into the conduction band of TiO2 than can be transferred from any other molecule. In contrast, a littlel Φinj , which may result from photo collisions, is seen in O6 owing to the huge gap between its absorption and emission spectra. After that, you may use Eq. to calculate the IPCE. (11):

$$IPCE = LHE \times \Phi_{inj} \times \eta_{collect}$$

As mentioned earlier, IPCE is the key factor determining the efficiency at which the dye can inject photoelectrons into the conduction band of TiO2. The large Φinj in O3 causes a large IPCE, whereas the small Φinj in O6 causes a very small IPCE. An electron can be efficiently transferred to the first excited state if it has a long lifetime (t), which is denoted by the equation:

$$t = \frac{1.499}{f \times E^2}$$

the unconstrained energy gained by injecting electrons ΔG^{regen}_{dye} can be expressed as:

$$\Delta G_{inject} = E^{dye*}_{Ox} = E^{dye}_{Ox} - E_{00}$$

which E dye the dye's ground-state oxidation potential, Ox, and the accompanying electronic vertical transition energy, E00 λmax. An important component that may influence the efficiency of photoelectric conversion is the rate of free-energy regeneration ΔG^{regen}_{dye} which can be written as:

$$\Delta G^{regen}_{dye} = E^{electrolyte}_{redox} - E^{dye}_{ox}$$

in which a high G regen dye may stimulate dye regeneration and boost JSC Since O4 had the greatest G regen dye value, its photoelectrons can be regenerated with less effort.'

Transition Density Matrix (TDM)

Analysis of electron-hole overlap () and charge-transfer lengths (r) during excitations may be seen on a spatial map provided by the transition density matrix (TDM) (Tables 4 and 5). The former refers to the distance between an electron and the matching hole in a semiconductor. To differentiate between LE and CT, this chemical index might be employed. This is the case if r 2 and the opposite if r > 2. Distance between electrons and holes is shown in Table 4 for the various orbital pairings. In terms of the electron-hole separation distance, Table shows that O4 > O3 > O2 > O5 > O1 > O7 > O6.

Table 4. Charge-transfer lengths (Δr) for the first excited state within each compound.

Compound	Δr (Å)	Orbital Pair
O1	3.31	242 → 251
O2	3.85	87 → 88
O3	3.98	91 → 92
O4	4.35	87 → 88
O5	3.12 3.38	159 → 165 161 → 165
O6	1.74	402 → 404
O7	2.26 2.89	213 → 217 216 → 217

Table 5 . Degree of electron–hole overlap (Λ) for the first excited state within each compound.

Compound	Λ	Orbital Pair
O1	0.324	242 → 251
O2	0.506	87 → 88
O3	0.471	91 → 92
O4	0.280	87 → 88
O5	0.150 0.118	159 → 165 161 → 165
O6	0.0476	367 → 404
O7	0.271 0.143	213 → 217 216 → 217

Given that LHE is a part of the IPCE, Φinj, We also compared r to ncollect, ncollect, and ncollect.

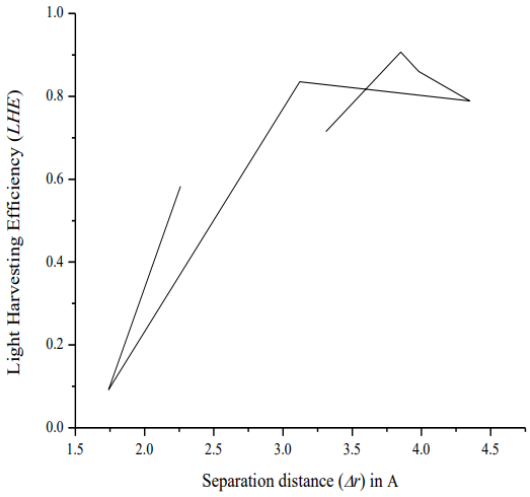

Figure 2. Graphical relationship between electron−hole separation distance and light-harvesting efficiency.

CONCLUSIONS

This study elucidated the efficacy of 1,3,4-oxadiazole moiety-containing compounds as metal-free organic dyes. The compounds were designed and optimized using DFT and TD-DFT. The compounds were employed as -spacer units inside each dye in dye-sensitized solar cells (DSSCs). Starburst, hydroxide, methoxy, amino, and triarylamine were all employed as donors, whereas cyano acrylic acid was used as an acceptor (save for O7). The results of IP and EA trials were consistent with one another. Studies of the compounds' anchoring regions using EA and MEP yielded consistent, acceptable results. The probability of charge recombination was calculated by studying electron-hole overlaps in isolated atoms and subatomic particles. The separation of electrons and holes was optimized by using charge-transfer lengths (r) as a chemical index. It was postulated that a smaller overlap between electrons and holes would lead However, the link between electron contributions and meant that this correlation did not hold up very well. The greatest r value was found in O4, and all of the compounds except O6 had r values over the threshold needed for charge transfer (CT) between their component atoms. There were fewer electrons in its anchoring groups compared to O6.

REFERENCES

1. Hua, T, Huang, ZS, Cai, K, Wang, L, Tang, H, Meier, H & Cao, D, 2019, 'Phenothiazine dye featuring encapsulated insulated molecular wire as auxiliary donor for high photovoltage of dye-sensitized solar cells by suppression of aggregation', Electrochim. Acta, vol. 302, pp. 225-233.
2. Irfan, A, 2019, 'Comparison of mono-and di-substituted triphenylamine and carbazole based sensitizers @ (TiO2) 38 cluster for dye-sensitized solar cells applications', Comput. Theor. Chem., vol. 1159, pp. 1-6.
3. Gnanasekar, S, Kollu, P, Jeong, SK & Grace, AN, 2019, 'Pt-free, lowcost and efficient counter electrode with carbon wrapped VO2 (M) nanofiber for dye-sensitized solar cells,' Sci. Rep., vol. 9.
4. Yoosuf, M, Pradhan, SC, Soman, S & Gopidas, KR, 2019, 'Triple bond rigidified anthracene-triphenylamine sensitizers for dyesensitized solar cells', Sol. Energy, vol. 188, pp. 55-65.
5. Fang, JK, Xu, M, Hu, X, Wu, C, Lu, S, Yu, HJ, Bao, X, Wang, Y, Shao, G & Liu, W, 2019, 'Aggregation-Free Organic Dyes Featuring Spiro [dibenzo cyclohepta quin
6. Zhang, J, Hao, Y, Yang, L, Mohammadi, H, Vlachopoulos, N, Sun, L & Hagfeldt, A, 2019, 'Electrochemically Polym.ized poly (3, 4- phenylenedioxythiophene) as efficient and transparent counter electrode for dye sensitized solar cells', Electrochim. Acta, vol. 300, pp. 482-488.
7. Zhang, J, Wang, Z, Li, X, Yang, J, Song, C, Li, Y, Cheng, J, Guan, Q & Wang, B, 2019, 'Flexible Platinum-Free Fiber-Shaped Dye Sensitized Solar Cell with 10.28% Efficiency', ACS Appl. Enr. Mater., vol. 2, pp. 2870-2877.
8. Zhang, L, Yang, X, Wang, W, Gurzadyan, GG, Li, J, Li, X, An, J, Yu, Z, Wang, H, Cai, B & Hagfeldt, A, 2019, '13.6% Efficient Organic Dye-Sensitized Solar Cells by Minimizing Energy Losses of the Excited State', ACS Enr. Let., vol. 4, pp. 943-951.
9. Zhang, R, Xu, J, Qian, J & Xia, J, 2019, 'Facile synthesis of poly (3, 4-ethylenedioxythiophene) and poly (bis-3, 4-ethylenedioxythiophene) via UV-irradiation Polym.ization and their reduction/iodine oxidation post-treatment for the application as counter electrodes for dyesensitized solar cells', Electrochim. Acta, vol. 313, pp. 505-512.
10. Zhu, H, Dong, Z, Pan, L, Han, Q, Niu, X, Li, J, Shen, K, Mai, Y, Li, Y & Wan, M, 2019, 'Investigation of Mo: Na and Mo related back contacts for the application in Cu (In, Ga) Se2 thin film solar cells', Solid-State Electr., vol. 157, pp. 48-54.
11. Wu, ZS, Guo, WJ, Zhang, J, Liu, YD, Song, XC, Jiang, Y, Weng, Q & An, ZW, 2019, 'Novel 4, 4′-bis (alkylphenyl/alkyloxyphenyl)-2, 2′- bithiophene bridged cyclic thiourea

functionalized triphenylamine sensitizers for efficient dye-sensitized solar cells', Sol. Energy , vol. 186, pp. 1-8. 124.

12. Xie, M, Hao, L, Jia, R, Wang, J & Bai, FQ, 2019, 'Theoretical study on the influence of electric field direction on the photovoltaic performance of aryl amine organic dyes for dye-sensitized solar cells', New J. Chem., vol. 43, pp. 651-661. 125.
13. Xie, X, Liu, Z, Li, W, Bai, FQ, Lee, EC & Zhang, HX, 2019, 'Theoretical study on organic dyes with tunable π-spacers for dyesensitized solar cells: Inspired by the organic Polymer photovoltaics', Chem. Phys. Let., vol. 719, pp. 39-44.
14. Xie, Y, Zhou, H, Zhang, S, Ge, C & Cheng, S, 2019, 'Influence of the auxiliary acceptor and π-bridge in triarylamine dyes on dye-sensitized solar cells', Photochem. Photobiol. Sci., vol. 18, pp. 2042-2051.
15. Xu, B, Wrede, S, Curtze, A, Tian, L, Pati, P, Kloo, L, Wu, Y & Tian, H, 2019, 'An Indacenodithieno [3, 2-b] thiophene based Organic Dye for Solid-state p-Type Dye-sensitized Solar Cells', ChemSusChem, vol. 12, pp. 3243-3248.

Corresponding Author

Meghmala Vaijanath Ingole*

Research Scholar, University Of Technology, Jaipur, Rajasthan.